OPEN ACCESS
Journal Homepage: http://ejournal2.undip.ac.id/index.php/jwl

JURNAL WILAYAH DAN LINGKUNGAN
P-ISSN: 2338-1604 dan E-ISSN: 2407-8751
Volume 14 Nomor 2, Agustus 2026, 197-219
https://doi.org/10.14710/jwl.14.2.197-219

Rapid Flood Mapping in Surabaya and Gresik using SAR and Optical Satellites: Leveraging Google Earth Engine for Timely Disaster Response

Zulfikar Adlan Nadzir[1]
Geomatics Engineering, Institut Teknologi Sumatera, Lampung, Indonesia

Mutia Rahma Apriani
Geomatics Engineering, Institut Teknologi Sumatera, Lampung, Indonesia

Muhammad Rohmaneo Darminto
Department of Geomatics Engineering, Institut Teknologi Sepuluh Nopember, Surabaya, Indonesia

Received : 3 April 2025
Accepted : 30 June 2026
Available Online : 31 August 2026

Abstract: Flooding in urban and semi-urban areas of Indonesia, particularly in Surabaya and Gresik, has become an ongoing challenge, exacerbated by rapid urbanization and climate change. This study explores the application of Sentinel-1 Dual-Polarization Water Index (SDWI) and Normalized Difference Water Index (NDWI) derived from Sentinel-2 and Landsat 9 imagery to map flood extents during three major flood events in 2022, 2023 and 2024. The analysis is conducted on a cloud-based Google Earth Engine (GEE) platform to enable near real-time flood monitoring with significantly faster processing time. The results indicate that NDWI is useful in detecting large-scale water bodies and coastal flooding, whereas SDWI performs better in urban and vegetated environments, capturing inundation in built-up areas that NDWI may overlook. The comparison of satellite-derived flood maps with ground-truth data from news reports confirms that both indices can provide indicative flood assessments where SDWI performs slightly better than NDWI. However, discrepancies between remote sensing data and ground observations suggest the need for a hybrid approach combining satellite data with ground-based observations to enhance flood mapping accuracy. The integration of these indices on cloud-based platforms like Google Earth Engine (GEE) offers a scalable solution for rapid flood mapping, supporting emergency response and disaster risk reduction efforts in Indonesia, particularly in flood-prone regions.

Keywords: Disaster Response, Flood Mapping, GEE, Indonesia, Optical, SAR

[1] Corresponding Author: Geomatics Engineering, Institut Teknologi Sumatera, Lampung, Indonesia
Email: zulfikar.nadzir@gt.itera.ac.id

How to Cite
Nadzir, Z. A., Apriani, M. R., & Darminto, M. R. (2026). Rapid Flood Mapping in Surabaya and Gresik using SAR and Optical Satellites: Leveraging Google Earth Engine for Timely Disaster Response. *Jurnal Wilayah dan Lingkungan, 14*(2), 197-219. https://doi.org/10.14710/jwl.14.2.197-219

Introduction

Climate change has fundamentally altered global weather cycles, exacerbating hydrometeorological disasters such as floods, especially in tropical and monsoon-affected regions like Indonesia (Eccles et al., 2019; Hariadi et al., 2024). Rising global temperatures plays a role to the intensification of precipitation regimes, increasing the occurrence and severity of extreme rainfall events (Calvin et al., 2023). In Indonesia, a country with complex river networks and rapid urban growth, these changes have led to high increase on frequency and impact of flooding, exacerbating socioeconomic vulnerabilities and infrastructural challenges (Hirabayashi et al., 2013; Loo et al., 2015). The unpredictability of extreme weather events highlight the increasing need for advanced and rapid flood monitoring and early warning systems, utilizing state-of-the-art technologies such as remote sensing and cloud-based geospatial analytics to enhance disaster response and mitigation strategies (Grimaldi et al., 2016; Munawar et al., 2022; Rahman & Di, 2017).

Historically, seasonal floods were largely driven by predictable monsoon cycles, but in recent decades, anthropogenic factors such as deforestation, land-use change, and poorly managed urban expansion have intensified flood risks (Djalante, 2018; Ward et al., 2013; Yamamoto et al., 2021). Major cities such as Jakarta, Surabaya dan Semarang are increasingly experiencing severe flood events, exacerbated by land subsidence and inadequate drainage infrastructure (Abidin et al., 2008, 2013; Chaussard et al., 2013; Erkens et al., 2015). For example, the December 2021 floods in Gresik submerged key districts like Driyorejo and Benjeng, blocking major roads and disrupting economic activity (Shofwan & Prabhaswara, 2023; Siswanto & Puspaningtyas, 2023). The impact of these floods extends beyond direct property damage, disrupting transportation networks, increasing disease outbreaks, and leading to economic losses in key sectors (Marfai et al., 2015; Nasution et al., 2022). Additionally, coastal areas face compounding threats from sea-level rise and storm surges, further amplifying the frequency and severity of extreme flooding events (Cao et al., 2021; Nicholls et al., 2021; Yin et al., 2020).

Recent advancements in satellite remote sensing and cloud-based computing have revolutionized flood monitoring and disaster response. Traditional flood assessments relied heavily on ground-based measurements and hydrodynamic models, which, while accurate, were often time-consuming and limited in spatial coverage. The advent of high-resolution Synthetic Aperture Radar (SAR) and optical satellite imagery—such as Sentinel-1, Sentinel-2, Landsat-9 and MODIS—combined with real-time data processing on platforms like Google Earth Engine (GEE) and NASA's SERVIR, now enables near-instantaneous flood mapping (Klemas, 2014; Rosser et al., 2017; Schumann & Moller, 2015; Simarmata et al., 2023; Twele et al., 2016). These technologies allow for the rapid identification of inundated areas, providing critical information for emergency response teams and policymakers. Particularly in Indonesia, where floods can develop rapidly due to extreme rainfall events, deforestation, and urbanization, there is a pressing need for fast and reliable flood mapping solutions. Remote sensing methods, when integrated with cloud-based platforms, can offer near real-time flood extent assessments, helping authorities make informed decisions on resource allocation and evacuation strategies (Avila-Aceves et al., 2023; Luu et al., 2020; Rehman et al., 2019). However, challenges such as cloud cover in optical imagery, SAR signal distortions in urban environments, and the need for high-quality training datasets persist, necessitating continued innovation in data processing techniques for improved flood detection accuracy, especially in flood-prone areas on the tropics (Antunes da Silva et al., 2024; Nguyen et al., 2022).

The Surabaya-Gresik region was selected for this study due to its high flood susceptibility and significant socio-economic impact. Located in East Java, Indonesia, this area experiences frequent coastal and riverine flooding, exacerbated by rapid urbanization, land subsidence, and extreme rainfall events. Several studies have identified Surabaya and

Gresik as flood-prone regions, with tidal flooding (locally known as *rob*) being a growing concern due to rising sea levels and land subsidence (Aulady et al., 2022). For example, a study in Gresik Regency utilizing the Analytical Hierarchy Process (AHP) and weighted overlay methods identified Driyorejo, Wringinanom, and Benjeng sub-districts as highly vulnerable to floods, with Driyorejo having 28.46 km^2 classified under high vulnerability (Taslyanto & Deviantari, 2024). Another study employed the Random Forest machine learning technique to assess flood vulnerability in Gresik, demonstrating the effectiveness of data-driven approaches in flood risk assessment (Arlisa & Handayani, 2023). Additionally, analysis of the Kali Lamong watershed, which spans Lamongan, Mojokerto, Gresik, and Surabaya, revealed that flooding remains a significant issue in Gresik due to the river's overflow (Santoso, 2013; Sholichin et al., 2024). These studies underscore the critical need for advanced flood mapping and management strategies in the Surabaya-Gresik area to mitigate the impact of recurrent flooding. This study employs two distinct methods for flood mapping—one based on water detection using spectral indices (e.g., Normalized Difference Water Index, NDWI) and another utilizing the backscatter of vegetation on the near-infrared band (e.g., SAR coherence analysis). By comparing their performance and accuracy, this research aims to provide insights into the most effective technique for rapid flood mapping in Indonesia. This study aims to develop and evaluate a rapid flood mapping framework that integrates remote sensing and cloud-based processing for near real-time flood extent estimation. Specifically, it seeks to assess the accuracy of different flood mapping methods and provide actionable flood extent information for disaster response agencies. The novelty of this study lies in its application of a comparative dual-method approach to a region with high flood variability while leveraging Google Earth Engine (GEE) for large-scale cloud-based analysis (Aggarwal, 2016; Aubrecht et al., 2013). Unlike previous studies that rely on a single flood mapping approach, this study evaluates the strengths and limitations of two different techniques, offering a more robust assessment of flood detection capabilities in Indonesia. The results of this research are expected to contribute to Indonesia's disaster management strategies by improving the speed and accuracy of flood assessments, ultimately supporting better risk mitigation and emergency response. Additionally, this study provides a methodological framework that can be replicated in other flood-prone regions, enhancing the global knowledge base on rapid flood mapping techniques.

Research Method

Study Area

This research focuses on the Surabaya-Gresik region in East Java as shown in **Figure 1**, an area highly vulnerable to seasonal and tidal flooding (*rob*). The location encompasses Indonesia's second-largest city, key economic hub and industrial port city. The research location is intersected by several major rivers e.g., Kali Lamong, Kali Mas, and Kali Surabaya as well as having recurrent tidal flooding on its coastal zones. This region serves as an important case study for evaluating rapid flood mapping techniques using remote sensing, as it represents a complex hydrological environment with urban, coastal, and riverine interactions.

Data

This study utilizes multisource remote sensing and ancillary datasets to assess flood dynamics in the Surabaya-Gresik region. These datasets include satellite imagery and geospatial layers, enabling a comprehensive analysis of flood extent and its impacts on infrastructure. The multi-temporal satellite data utilized for this study are from Sentinel-1 SAR satellite and from the optical sensor of Sentinel-2 and Landsat-9 satellite on the research location in three dates after significant floods, listed in **Table 1**: 1) 6th of July 2022,

2) 7th of December 2023, and 3) 7th of February 2024. The SAR imageries consist of both VV (vertical-vertical) and VH (vertical-horizontal) polarization as base bands so that it could be treated further as multispectral satellite imagery while the optical imageries consist of all available bands (red-green-blue, near-infrared, short-wavelength infrared and others). These remote sensing datasets are used to detect flood extent, duration, and recurrence patterns, allowing for comparative evaluation of flood mapping methods. Land cover classifications, road network maps and building footprints are obtained from the Indonesian Geospatial Agency (BIG – *Badan Informasi Geospasial*; https://tanahair.indonesia.go.id/). The usage of geospatial layers stems from the fact that floods in research location have been found to have severe consequences on critical infrastructure (Cahyono et al., 2021; Sari et al., 2021), such as transportation disruption on Cerme and Driyorejo on July 2022, disruption on economy due to flooded industrial zone and Tanjung Perak Port on December 2023, disease outbreaks and electricity shutdowns in Driyorejo, Wringinanom and Benjeng on July 2022, and damage on drainage system on Surabaya's coastal zones on February 2024.

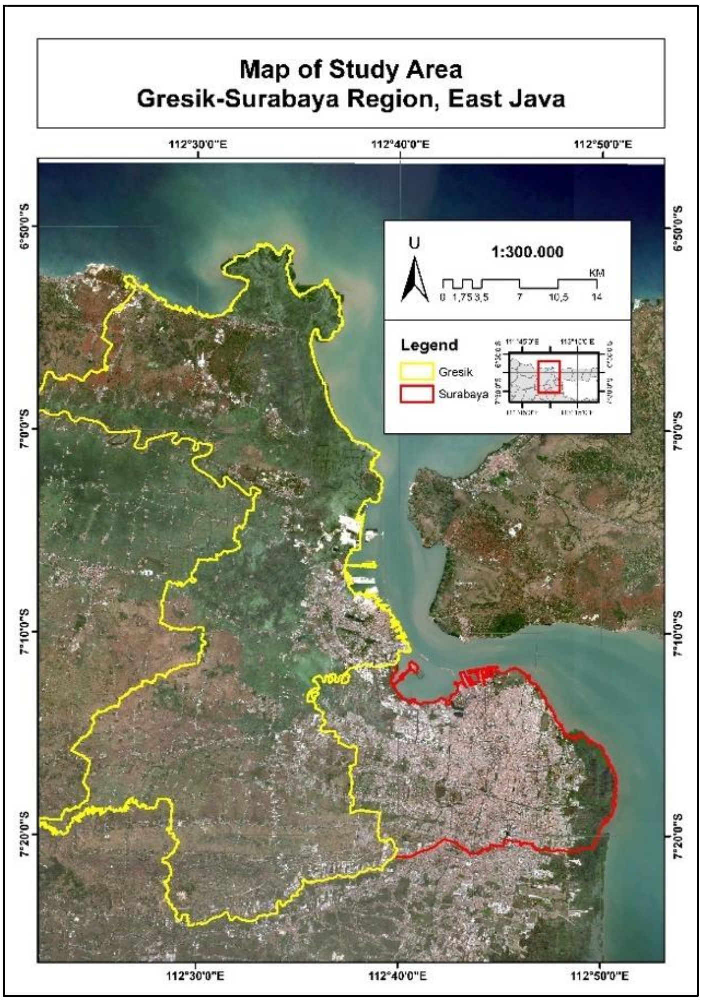

Source: Authors, 2025

Figure 1. Study Area

Table 1. Observation Time and Explanation of Remotely sensed Data

Date of Flood	Satellite	Acquisition Date
6^{th} of July 2022	Sentinel-1	7^{th} of July 2022
	Sentinel-2	7^{th} of July 2022
7^{th} of December 2023	Sentinel-1	9^{th} of December 2023
	Landsat-9	7^{th} of December 2023
7^{th} of February 2024	Sentinel-1	7^{th} of February 2024
	Landsat-9	9^{th} of February 2024

Source: Author's analysis, 2025

It should be noted that the satellite acquisition dates do not always coincide exactly with the reported flood dates. The temporal gap between the reported flood occurrence and the remotely sensed observations ranges from the same day to two days after the event. The 6 July 2022 flood was represented by Sentinel-1 and Sentinel-2 observations acquired on 7 July 2022; the 7 December 2023 flood was represented by Landsat-9 imagery acquired on the same day and Sentinel-1 imagery acquired on 9 December 2023; while the 7 February 2024 flood was represented by Sentinel-1 imagery acquired on the same day and Landsat-9 imagery acquired on 9 February 2024. Therefore, the mapped inundation should be interpreted as post-event observable flood extent rather than the exact maximum flood extent at the time of peak inundation. To reduce this temporal uncertainty, the satellite-derived flood maps were compared with curated news reports that provided spatial information on affected sub-districts, roads, settlements, and infrastructure around the corresponding flood periods.

Methodology

This research employs a remote sensing-based flood mapping approach using spectral indices and SAR-based analysis, integrated within a cloud-based computing platform with news articles-based validation. The methodology consists of three main stages as indicated on **Figure 2**: (1) Data Collection and Preprocessing, (2) Flood Mapping using NDWI and SDWI (Sentinel-1 Dual-Polarized Water Index), and (3) Accuracy Assessment by means of Confusion Matrix and Impact Analysis using waterbody and flooded road as two main parameters.

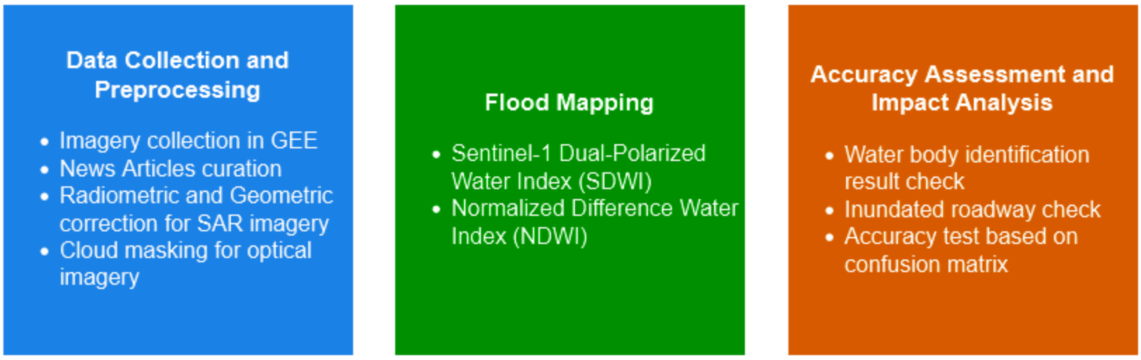

Source: Authors, 2025

Figure 2. Research Flowchart

First step on the initial stage of data collection and preprocessing is to collect all associated data on their respective sources, in addition to utilize Google Earth Engine (https://earthengine.google.com/) as the platform to collect, filter and process the satellite data, with the particular advantage that no download and upload are needed, simplifying and speeding up the whole process. Meanwhile, several news articles on the topic of the flood in research area were curated and reviewed to get a robust validation dataset based on the location mentioned on these articles.

Initial pre-processing on the SAR data was focused on the geometry correction, started by computing look angle and elevation angle to adjust the orientation of the radar antenna to be in-line with the Earth's surface. Additionally, range resolution (represents the ability to distinguish two different object parallel to the flight direction), azimuth resolution (similar to range resolution but perpendicular to the flight direction) and range (distance between radar antenna and the Earth's surface) was computed to quantify the spatial resolution of the data (Yu et al., 2020; Zhu & Bamler, 2014). Due to SAR main disadvantage of high error caused by atmosphere condition and topography effect on the radar beam (commonly termed as layover or shadow effect), second step on SAR pre-processing was to estimate two main parameters. The first one is called model geometry that represents the topographical situation on the location while the second one is called volumetric model, where the behavior and interaction between the radar pulse with the Earth's surface was computed. Both parameters were utilized to approximate the corrected radar pulse feedback that describes the radar behavior on the flattened Earth's surface. The third and last step on the SAR pre-processing was to focus on the radiometry part, since the SAR data tends to have salt and pepper-like pattern—commonly called speckle—on the image because of the constructive and destructive nature of backscatter waves on identical target with different arbitrary phase (Chen, 2020). A filter called focal-median that utilizes the median value of a group of pixels in a circle, represented in **Equation 1** (Castaneda et al., 2021) with g as noisy imagery, k as kernel circle size, $\hat{g}$ as de-noised image and i as the index of pixel. This filter is more advantageous than others since it was relatively simple yet robust in preserving the edges and relatively quick in processing time (Kupidura, 2016).

$$\boxed{f(g,k) = \hat{g} = \frac{(\hat{g} + [median(g,[2i-1]^2)]}{2}, i++} \tag{1}$$

The performance of an optical remote sensing sensor is highly dependent on the weather condition in the form of existence of cloud cover. Most datasets available on the GEE provide dedicated band(s) for cloud identification and cloud masking, two of them are Sentinel-2 Level 2A (cloud and cloud_shadow) and Landsat Collection 2 Top of Atmosphere Data (cloud_confidence and cloud_shadow). These bands are utilized to mask the cloud out of the multi-temporal optical imagery of respective dataset as the pre-processing step.

Flood mapping started with the estimation of SDWI on Sentinel-1 imagery. Sentinel-1 itself consists of two polarizations (VV and VH) that differ in the backscatter intensity pattern (Sun et al., 2020). The VV is sensitive to identify water, while the VH is suitable to detect build-up areas. This difference stems from the polarization axis, where both emitted and reflected pulse is on vertical axis for VV while the reflected pulse of VH is on horizontal axis (Xue et al., 2021). Additionally, the low radar reflectance of water compared to land reflectance was utilized, as indicated in **Equation 2** (Simarmata et al., 2023). SDWI ranges between -1 to 1, with positive value indicates the existence of waterbody and negative value represents land surface. Results of SDWI were then utilized as a binary mask (water or no water; 1 or 0) to extract and highlight the location of waterbodies or inundated areas.

$$\boxed{SDWI = \frac{(VV - VH)}{(VV + VH)}} \tag{2}$$

Similarly, NDWI algorithm that estimates the occurrence of waterbody is utilized on both Sentinel-2 and Landsat imagery. The NDWI itself was based on the difference on reflectance of near-infrared (NIR) and green (G) band that is sensitive to waterbody, as indicated on **Equation 3** (Singh & Kansal, 2022). Then, to conduct a proper segmentation, a threshold value is adapted from (Ahmed & Akter, 2017) with value of 0 where it was based on manual histogram thresholding on the NDWI results. As a comparison, the threshold on SDWI result is adapted from (Guo et al., 2021; Ta et al., 2024) with value of 0.2 as the choice after a definitive check and adjustment on the histogram.

$$\boxed{NDWI = \frac{(G - NIR)}{(G + NIR)}} \quad (3)$$

In order to evaluate the reliability and performance of both flood mapping methods and data sources, an accuracy assessment is performed using confusion matrix-based metrics (e.g., Overall Accuracy [OA], Producer's, and User's Accuracy) as shown in **Equation 4** by comparing detected flood areas with reference data from curated news reports (Sadiq et al., 2022; Schnebele & Cervone, 2013) with TP or Total Positive as number of correctly classified intended positive class while TN or Total Negative as number of correctly classified negative class. Furthermore, an impact analysis is conducted by overlaying flood extent maps with infrastructure layers (roads, settlements, industrial zones) to assess affected road networks, inundated settlement area and ability to detect persistent waterbody in the area.

For the accuracy assessment, 44 validation points were selected for each flood event using a purposive, spatially constrained sampling approach. The points were not generated as purely random samples, because the validation relied on spatial information extracted from curated news reports, visual interpretation of high-resolution basemap imagery, and the availability of identifiable flooded and non-flooded locations. The validation points were distributed across reported flood-affected and non-affected locations in Surabaya and Gresik, including urban settlements, industrial areas, road corridors, bridge locations, coastal zones, and river-adjacent areas along the Kali Lamong and Kali Mas floodplain. Flooded points were assigned where news reports or visual interpretation indicated inundation near the corresponding satellite acquisition period, while non-flooded points were selected from nearby areas with no reported flooding and no visible inundation signature. This procedure was designed to provide a practical event-based validation dataset; however, it should be interpreted as a limited purposive validation sample rather than a statistically representative probability sample.

$$\boxed{\text{OA} = {TP + TN}/_{Sample\ Size}} \quad (4)$$

Results and Discussions

News articles-based curation of flood events

Flooding remains a persistent issue in Surabaya and Gresik, with significant events occurring on 6 July 2022, 7 December 2023, and 7 February 2024. These floods resulted in widespread infrastructure damage, particularly affecting transportation networks, residential areas, and industrial zones. On 6 July 2022, severe rainfall overwhelmed drainage systems, leading to the inundation of key roads in Tandes, Surabaya, and Sidayu and Panceng in Gresik (Pusat Krisis Kesehatan, 2022), causing extensive traffic disruptions. The 7 December 2023 event, exacerbated by high tides, led to severe flooding in Balongpanggang, Benjeng and Cerme sub-districts in Gresik, with several bridges and local markets submerged. Additionally, several sub-districts in Surabaya were flooded (e.g., Asem Rowo, Benowo, Dukuh Pakis, Tandes, Wiyung, Wonokromo, Bubutan, Gubeng, Sawahan, Simokerto, Sukomanunggal, Tegal Sari, Wonocolo) (Karnaji et al., 2024). Meanwhile, the 7 February 2024 flood was linked to the overflow of Kali Lamong and Kali Mas River, severely impacting Gresik's industrial zones and Surabaya's settlement areas, where factories halted operations due to floodwater intrusion, highlighting the economic consequences of recurring inundation. These events underscore the critical need for accurate and rapid flood mapping to support emergency response and mitigation efforts, particularly in urban and semi-urban areas where land-use changes and drainage capacity issues exacerbate flood risks. The curation of news articles as validation sources has shown to be an effective means of cross-verifying flood impacts reported in satellite-derived data (Rosser et al., 2017; Yagoub et al., 2020).

SDWI and NDWI Results and Impact Analysis on Settlements and Road Network

The application of Sentinel-1 Dual-Polarization Water Index (SDWI) and Normalized Difference Water Index (NDWI) provides a detailed spatial assessment of flood extent in Surabaya-Gresik across the three major flood events. NDWI, derived from Sentinel-2, Landsat 8 and Landsat 9 MSI (multispectral) imagery, effectively identifies surface water features by leveraging the contrast between near-infrared (NIR) and green band reflectance. However, NDWI tends to overestimate flood extent due to the presence of built-up areas and vegetation with high moisture content. In contrast, SDWI enhances flood detection in complex environments, particularly urban and semi-urban areas where mixed land covers complicate classification (Kuenzer et al., 2013; Uddin et al., 2019).

The flood maps generated from NDWI and SDWI for (a) 6 July 2022, (b) 7 December 2023, and (c) 7 February 2024 as shown in **Figure 3** and **Figure 4**, indicated similar spatial patterns and inundated locations across the events and indices. These results indicate persistent inundation occurred in low lying sub-districts of Surabaya (e.g. Asem Rowo, Benowo, Tandes) as well as sub-districts in Gresik located on the Kali Lamong and Kali Mas basin (such as Cerme, Benjeng, Menganti and Driyorejo). The February 2024 event exhibited the most extensive flooding, with NDWI indicating an increase in surface water cover by approximately 45% compared to dry-season baselines, while SDWI results captured additional inundation in built-up and vegetated areas not detected by NDWI alone. All three flood occurrences, primarily driven by river overflow on the southwest Gresik part, showed higher water depths along the Kali Lamong and Kali Mas basin, with NDWI and SDWI confirming a southward flood progression towards industrial zones in Gresik as well as port area in Surabaya (Aprillya & Chasanah, 2021; Fristyananda & Idajati, 2017; Triana & Hidayah, 2020). Additionally, it could be seen that the distribution of inundated areas from NDWI is denser than the SDWI, leading it to have significantly larger total inundated areas (~4 to 5 times bigger), listed on **Table 2**. This overestimation by NDWI is particularly pronounced in coastal and urban regions, where high moisture content in vegetation and infrastructure may be misclassified as water. Conversely, SDWI provides a more conservative flood estimate, which aligns more closely with observed flooding in industrial and settlement areas. These results demonstrate the complementary nature of NDWI and SDWI in flood mapping, with NDWI excelling in detecting open water bodies especially close to the coast and SDWI improving detection in vegetated and urban regions. This approach enhances the reliability of rapid flood assessments, which is crucial for supporting emergency response strategies in high-risk urban flood zones like Surabaya-Gresik area.

The temporal gap between flood occurrence and satellite acquisition is an important consideration in interpreting these results. For the July 2022 event, both Sentinel-1 and Sentinel-2 were acquired one day after the reported flood date, suggesting that the detected inundation represents residual floodwater that remained observable after the initial event. For the December 2023 event, the Landsat-9 image was acquired on the same day as the reported flood, while the Sentinel-1 image was acquired two days later; thus, the NDWI result is more likely to approximate the immediate flood condition, whereas the SDWI result may reflect persistent inundation in low-lying or poorly drained areas. For the February 2024 event, Sentinel-1 was acquired on the same day, while Landsat-9 was acquired two days later, meaning that the SDWI result is temporally closer to the reported flood occurrence, while the NDWI result may represent remaining inundation after partial recession. The persistence of flooding is supported by the spatial agreement between the satellite-derived inundation and curated news reports, particularly in repeatedly affected areas. However, because floodwater can recede rapidly in urban drainage systems, these maps should be interpreted as as satellite-observed inundation during the acquisition windows.

Table 2. Inundated Area from NDWI and SDWI for the 3 flood events

Date of Flood	NDWI Area (km^2)	SDWI Area (km^2)
6th of July 2022	1.0947	1.0134
7th of December 2023	3.7427	0.7571
7th of February 2024	5.9957	1.2005

Source: Author's analysis, 2025

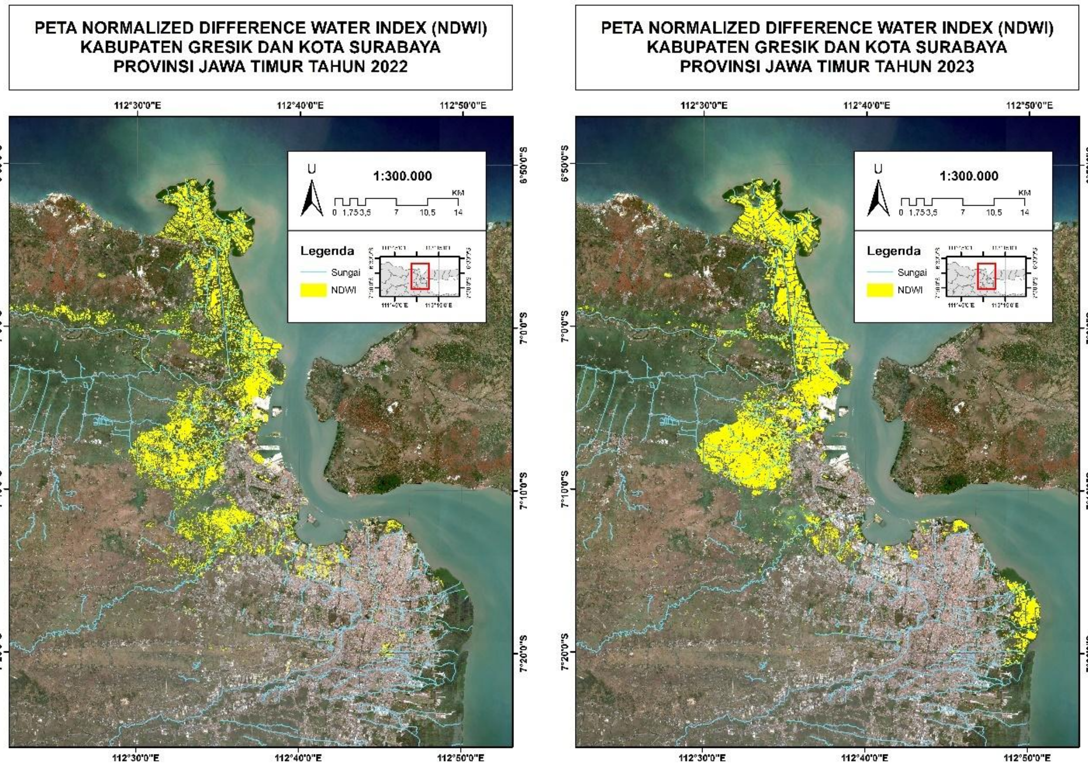

(a) (b)

https://doi.org/10.14710/jwl.14.2.197-219

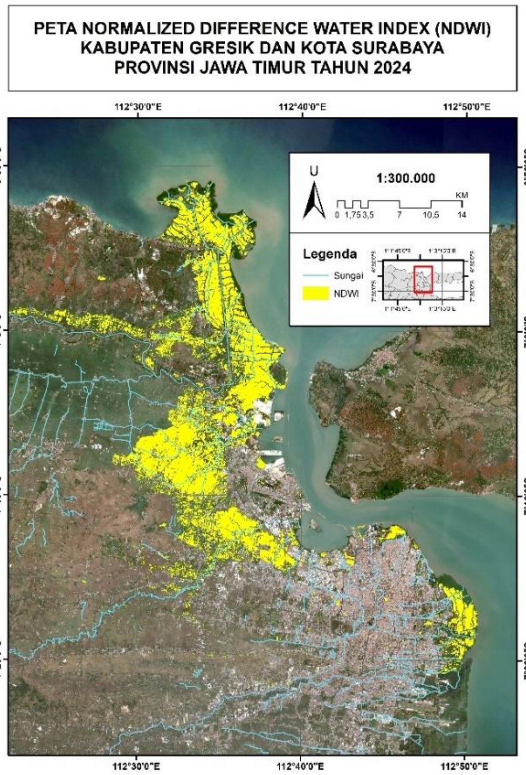

(c)

Source: Authors, 2025

Figure 3. NDWI Map of (a) 6 July 2022, (b) 7 December 2023, and (c) 7 February 2024 flood

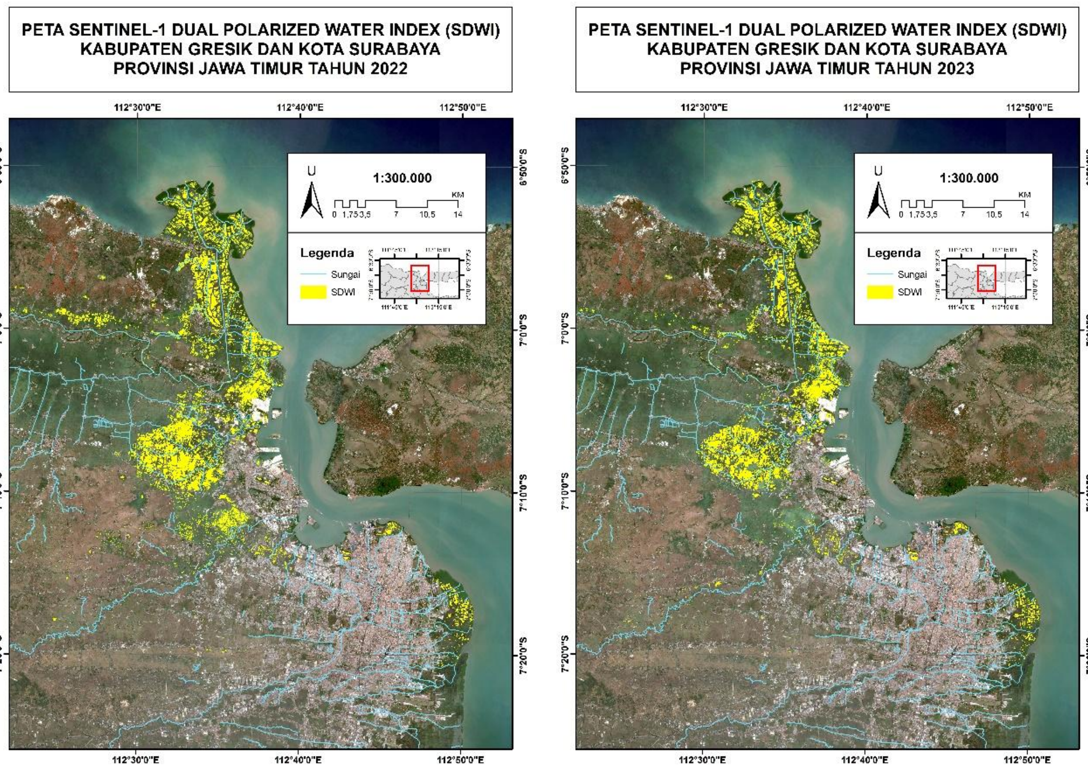

(a) **(b)**

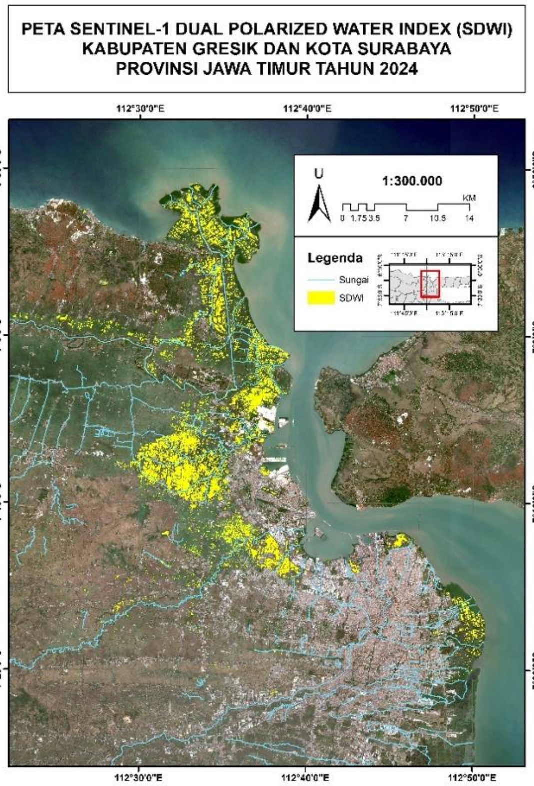

(c)

Source: Authors, 2025

Figure 4. SDWI Map of (a) 6 July 2022, (b) 7 December 2023, and (c) 7 February 2024 flood

The integration of NDWI and SDWI provides a robust methodology for identifying flood-affected areas, particularly distinguishing permanent water bodies around dense built-up areas in Surabaya-Gresik. Three permanent water bodies (Krembangan Viaduct, Ngipik Pond and Bunder Reservoir) and two flood-prone bridges on Kali Lamong and Kali Mas (Sembayat and Boboh Bridge) were the subject to a detailed analysis as shown in **Table 3**. NDWI maps clearly delineate Kali Mas and Kali Lamong, while SDWI enhances the identification of standing body of water close to settlements and bridges, which are often misclassified in NDWI due to urban infrastructure in the surroundings (Malinowski et al., 2015; Martinis & Rieke, 2015). This misclassification could be exacerbated by the loss of information due to the cloud masking preprocessing on the optical remote sensing data, one of the disadvantage of the sensor compared to the SAR data (Nadzir et al., 2020).

The flood extent comparison with news-reported flood locations validates the accuracy of satellite-derived flood mapping, as shown in **Figure 5.** It quantifies the intersection between inundated areas with settlements land-use from the BIG using overlay tool. For instance, the July 2022 flood was reported to have severely impacted on residential zones in Sidayu and Panceng (Gresik) and industrial parks in Tandes, Surabaya, which corresponds well with the inundation detected by SDWI and NDWI. The December 2023 as well as February 2024 flood, which was primarily driven by river overflow, showed extensive water spread along the Kali Lamong and Kali Mas floodplain, with both indices confirming flooding in Benjeng, Cerme, and parts of western Surabaya. Additionally, ground-level images from news reports and social media indicate water levels exceeding 50 cm in some residential areas, corroborating SDWI's enhanced sensitivity to shallow water bodies. The discrepancies between the satellite-derived and news-reported flood extents highlight both the strengths and limitations of each approach. While remote sensing enables large-scale rapid mapping, ground reports provide crucial context regarding localized inundation depth, infrastructure damage, and evacuation efforts. This emphasizes the need for a hybrid approach that integrates satellite data, ground observations, and crowdsourced flood information to improve flood response strategies in Indonesia (Assumpção et al., 2018; See, 2019; Sy et al., 2019).

Table 3. Comparison between SDWI and NDWI on several features

Imagery	Feature	NDWI	SDWI
		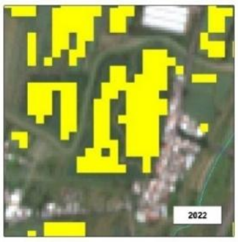	
	Boboh Bridge	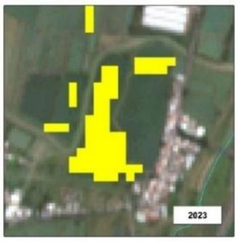	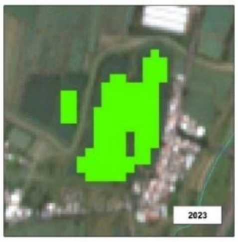
		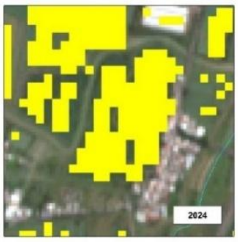	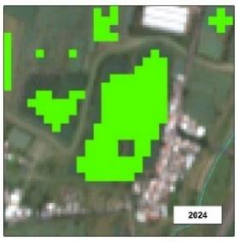
			
	Sembayat Bridge		
			

Imagery	Feature	NDWI	SDWI
		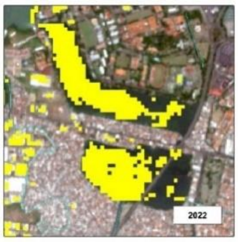	
	Krembangan Viaduct		
			
			
	Ngipik Pond		
			
	Bunder Reservoir		

Imagery	Feature	NDWI	SDWI
			
		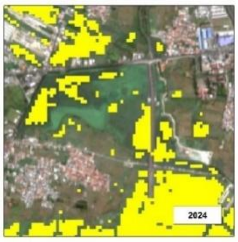	

Source: Author's analysis, 2025

Beyond assessing flood extent in settlements and industrial zones, the results also highlight the impact on critical road networks in Surabaya and Gresik, as shown in **Figure 6**. Results show that despite the detailed visual check, no significant blockade was detected. This was mainly due to the resolution of remote sensing imagery utilized in this study, which are 10 meters for Sentinel-1 and 30 meters for Sentinel-2 and Landsat 9, while the average road width on the research location was 3.5 meters.

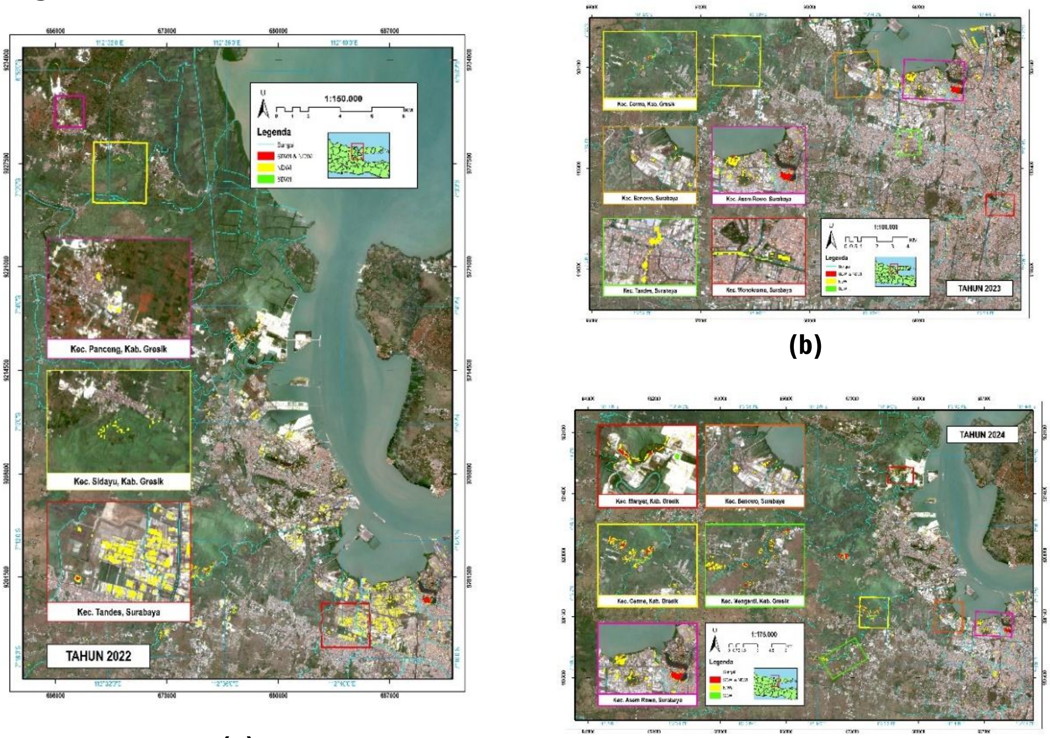

(a) (b) (c)

Source: Authors, 2025

Figure 5. Inundated Settlement Map of (a) 6 July 2022, (b) 7 December 2023, and (c) 7 February 2024 flood

NDWI	SDWI

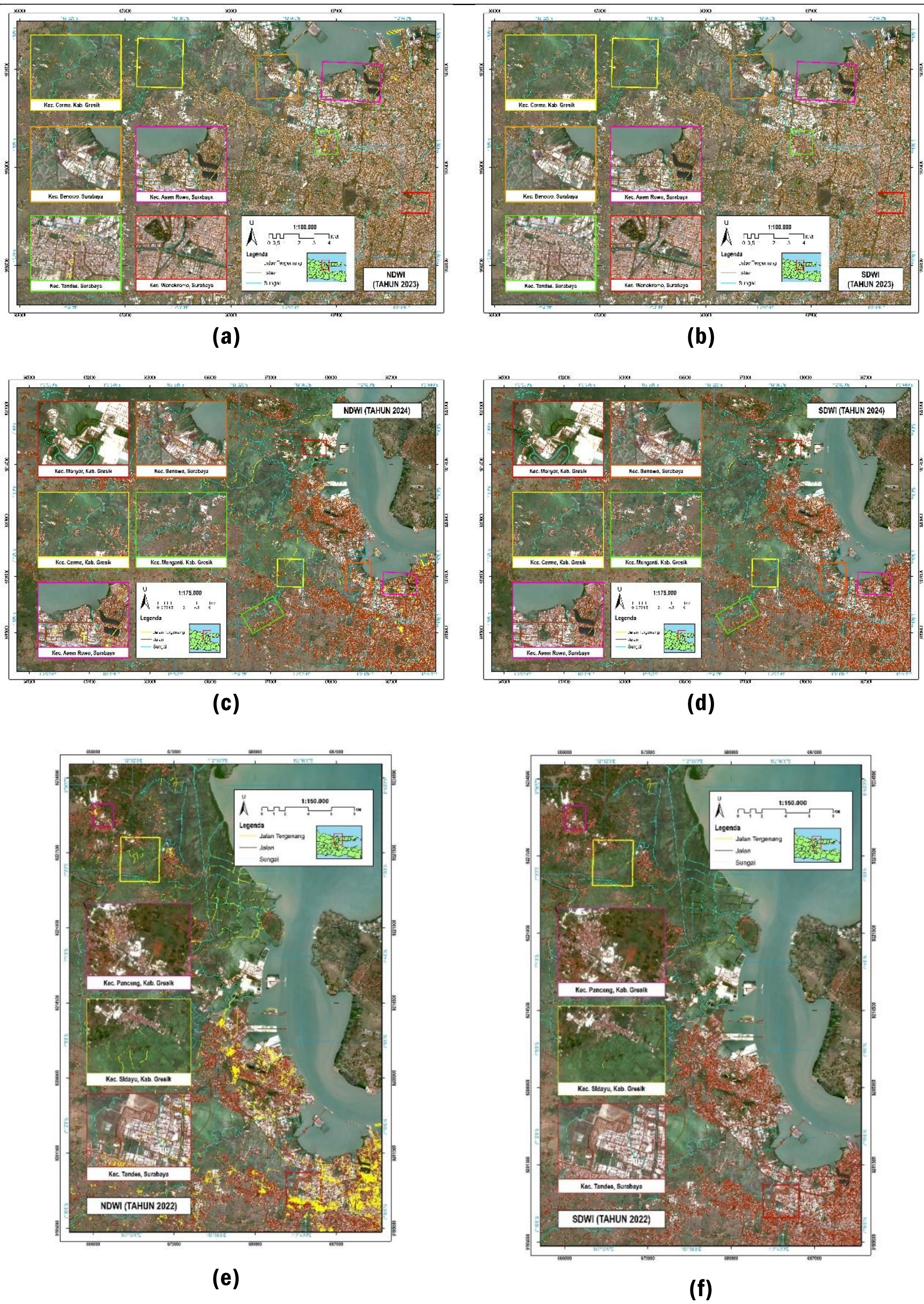

Source: Authors, 2025

Figure 6. Inundated Road Network Map of, (a and b) 7 December 2023, (c and d) 7 February 2024, and (e and f) 6 July 2022 flood

Accuracy Assessment and Implications for Rapid Flood Mapping in Indonesia

To evaluate the performance of NDWI and SDWI, a confusion matrix-based accuracy assessment was conducted using ground-truth flood extent data derived from news reports and visual interpretation of high-resolution imagery. The overall accuracy and kappa coefficient were calculated to determine the agreement between the remote sensing-based flood detection methods and independent reference data, shown in **Table 4**, **Table 5** and **Table 6** for each flood event. Results indicate that SDWI slightly edges NDWI in identifying inundated settlements for all three flood events (having better overall accuracy of 52.57% compared to 50% in average), particularly in urban areas where mixed land cover types often lead to misclassification in traditional water indices (Chini et al., 2017; Zhao et al., 2024). NDWI, however, provided better delineation of large-scale waterbodies and on coastal plain, making it useful for detecting major river overflow and extensive flood events (Atefi & Miura, 2022; Farhadi et al., 2024, 2025). The confusion matrix analysis further revealed higher commission errors in NDWI, particularly in areas with shallow flooding and urban structures, whereas SDWI exhibited lower omission errors due to its sensitivity to wet surfaces. In other words, the NDWI found to overestimate the flood extent while the SDWI is more restrictive on identifying inundated areas. The December 2023 flood event, for instance, saw NDWI miscalculating the extent of inundation in Gresik's industrial zones, while SDWI effectively captured these areas as flooded, aligning well with reported affected infrastructure. However, NDWI remains crucial for detecting large-scale river overflow and coastal flooding, as evidenced by the February 2024 flood event. Despite the advantages of both indices, their accuracy remains moderate, with overall accuracy ranging from 36% to 52%. These findings suggest that a multi-index approach, integrating NDWI for large-scale flood detection and SDWI for urban flood analysis, could significantly improve flood mapping accuracy in complex environments (Muñoz et al., 2021; Soria-Ruiz et al., 2022; Tanim et al., 2022). However, the accuracy results should be interpreted with caution because the validation sample is relatively small and imbalanced, especially for the 2022 event, where only 3 of the 44 validation points were classified as flooded in the reference data. This imbalance limits the reliability of class-specific accuracy estimates for the flooded class and can cause overall accuracy to be dominated by the non-flooded class. The number of validation points could not be substantially increased because the available news reports did not consistently provide spatially precise flood information. Many reports described flooding only at the administrative-unit level, such as sub-districts, villages, road names, or general landmarks, without providing coordinates, flood boundaries, water depth distribution, or clear distinction between flooded and non-flooded areas. Several reports also referred to the same locations across different media outlets, resulting in duplicate spatial information rather than additional independent validation points. In addition, some reported locations could not be confidently matched to a specific pixel or spatial feature in the satellite imagery because of ambiguity in place names, rapidly changing flood conditions, or insufficient visual evidence. Therefore, only locations that could be spatially identified with sufficient confidence from news descriptions, high-resolution basemap interpretation, and proximity to reported flood impacts were retained as validation points. This constraint is acknowledged as a major limitation of the validation design.

Table 4. Confusion Matrix of SDWI and NDWI for 2022 flood

Classification Result	Field		Row Sum	Producer Accuracy	User Accuracy	Overall Accuracy
	Flooded	Not Flooded				
NDWI						
Flooded	3	38	41	100.00%	7.32%	13.64%
Not Flooded	0	3	3	7.32%	100.00%	
Column Sum	3	41	44			

Classification Result	Field Flooded	Field Not Flooded	Row Sum	Producer Accuracy	User Accuracy	Overall Accuracy
			SDWI			
Flooded	2	20	22	66.67%	9.09%	52.57%
Not Flooded	1	21	22	51.22%	95.45%	
Column Sum	3	41	44			

Source: Author's analysis, 2025

Table 5. Confusion Matrix of SDWI and NDWI for 2023 flood

Classification Result	Field Flooded	Field Not Flooded	Row Sum	Producer Accuracy	User Accuracy	Overall Accuracy
			NDWI			
Flooded	15	27	42	93.75%	35.71%	36.36%
Not Flooded	1	1	2	3.57%	50.00%	
Column Sum	16	28	44			
			SDWI			
Flooded	7	18	25	43.75%	28.00%	38.64%
Not Flooded	9	10	19	35.71%	52.63%	
Column Sum	16	28	44			

Source: Author's analysis, 2025

Table 6. Confusion Matrix of SDWI and NDWI for 2024 flood

Classification Result	Field Flooded	Field Not Flooded	Row Sum	Producer Accuracy	User Accuracy	Overall Accuracy
			NDWI			
Flooded	22	22	44	100.00%	50.00%	50.00%
Not Flooded	0	0	0	N/A	N/A	
Column Sum	22	22	44			
			SDWI			
Flooded	12	11	23	54.55%	52.17%	52.27%
Not Flooded	10	11	21	50.00%	52.38%	
Column Sum	22	22	44			

Source: Author's analysis, 2025

One limitation of this study is the temporal mismatch between reported flood occurrence and satellite acquisition time. Although the acquisition gap was relatively short, ranging from zero to two days, flood extent in urban and semi-urban environments can change rapidly due to drainage, river discharge variation, tidal influence, and local pumping or runoff conditions. As a result, the satellite-derived flood maps may underestimate areas that were flooded during the peak event but had already receded before image acquisition, or may emphasize areas where inundation persisted longer due to low topography and poor drainage. In the absence of continuous hydrological gauge or water-level data for all affected locations, curated news reports were used as the primary spatial validation source. This approach provides valuable ground-context information, but it also introduces uncertainty because news reports may be spatially incomplete, unevenly distributed, and biased toward populated or highly impacted areas. Therefore, the results should be interpreted as rapid post-event flood mapping products rather than complete reconstructions of maximum flood extent.

The findings of this study have direct implications for disaster response and mitigation in Indonesia. Given the frequency and severity of flooding in coastal and riverine cities like Surabaya and Gresik, the integration of NDWI and SDWI on cloud-based platforms such as Google Earth Engine (GEE) offers a scalable and near real-time solution for rapid flood mapping. This can enhance disaster preparedness efforts by providing emergency responders with timely and accurate flood extent information (Kim et al., 2022; Li et al., 2024). Moreover, the integration of remote sensing with news-based validation provides an additional layer of ground-truthing, ensuring that flood maps reflect real conditions on the ground. Ultimately, this research contributes to Indonesia's broader disaster risk reduction efforts, supporting data-driven decision-making in flood-prone regions and improving resilience against climate-induced extreme events.

Conclusions

This study has demonstrated the effectiveness of Sentinel-1's Dual-Polarization Water Index (SDWI) and Sentinel-2's and Landsat 9's Normalized Difference Water Index (NDWI) in mapping flood extents in Surabaya and Gresik, Indonesia, during three significant flood events (6 July 2022, 7 December 2023, and 7 February 2024). The results highlight the complementary strengths of both indices, where NDWI excels in detecting large water bodies and coastal flooding, while SDWI enhances flood detection in urban and semi-urban areas, particularly in built-up and vegetated environments. The comparison with ground-truth data from news reports and high-resolution imagery confirms the utility of these indices in providing timely and accurate flood mapping. However, discrepancies between the flood maps and news-reported locations also suggest that combining satellite data with ground-based observations and crowdsourced information is crucial for improving the accuracy and reliability of flood mapping efforts. The integration of NDWI and SDWI offers a robust framework for rapid flood assessment, supporting decision-making in flood-prone regions like Surabaya and Gresik. The results also emphasize the importance of utilizing cloud-based platforms such as Google Earth Engine (GEE) for near-real-time flood monitoring, enhancing disaster response and mitigation strategies in Indonesia. In conclusion, the study provides valuable insights into the potential of satellite-derived indices for flood mapping and lays the foundation for future improvements in flood monitoring systems in Indonesia.

Moving forward, the fusion of multiple indices such as NDWI and SDWI, along with advanced machine learning techniques, holds great promise for improving flood mapping accuracy. Further research is needed to refine thresholds for different land-cover types and enhance the capabilities of these indices in urban flood assessments. Additionally, integrating high-resolution imagery and crowdsourced data will strengthen the overall flood monitoring framework in Indonesia, contributing to more resilient flood management systems in the face of climate change-induced extreme events.

References

Abidin, H. Z., Andreas, H., Djaja, R., Darmawan, D., & Gamal, M. (2008). Land subsidence characteristics of Jakarta between 1997 and 2005, as estimated using GPS surveys. *GPS Solutions*, *12*(1), 23–32. https://doi.org/10.1007/s10291-007-0061-0

Abidin, H. Z., Andreas ,H., Gumilar ,I., Sidiq ,T.P., & and Fukuda, Y. (2013). Land subsidence in coastal city of Semarang (Indonesia): Characteristics, impacts and causes. *Geomatics, Natural Hazards and Risk*, *4*(3), 226–240. https://doi.org/10.1080/19475705.2012.692336

Aggarwal, A. (2016). Exposure, hazard and risk mapping during a flood event using open source geospatial technology. *Geomatics, Natural Hazards and Risk*, *7*(4), 1426–1441. https://doi.org/10.1080/19475705.2015.1069408

Ahmed, K. R., & Akter, S. (2017). Analysis of landcover change in southwest Bengal delta due to floods by NDVI, NDWI and K-means cluster with landsat multi-spectral surface reflectance satellite data. *Remote Sensing Applications: Society and Environment*, *8*, 168–181. https://doi.org/10.1016/j.rsase.2017.08.010

Antunes da Silva, L., Rudorff, C., Ovando, A., Pimentel, A., Cuartas, L. A., & dos Santos Alvalá, R. C. (2024). Inundation mapping using hydraulic modeling with high-resolution remote sensed data: A case study in the Acre River Basin, Brazil. *Modeling Earth Systems and Environment*, *10*(3), 3051–3066. https://doi.org/10.1007/s40808-024-01972-x

Aprillya, M. R., & Chasanah, U. (2021). Analisis Lahan Pertanian Rawan Banjir Menggunakan Metode Multi Atribut Utility Theory Berbasis Sistem Informasi Geografis. *Informatika Mulawarman : Jurnal Ilmiah Ilmu Komputer*, *16*(2), 148. https://doi.org/10.30872/jim.v16i2.6554

Arlisa, S. D., & Handayani, H. H. (2023). Flood Vulnerability Analysis using Random Forest Method in Gresik Regency, Indonesia. *IOP Conference Series: Earth and Environmental Science*, *1127*(1), 012023. https://doi.org/10.1088/1755-1315/1127/1/012023

Assumpção, T. H., Popescu, I., Jonoski, A., & Solomatine, D. P. (2018). Citizen observations contributing to flood modelling: Opportunities and challenges. *Hydrology and Earth System Sciences*, *22*(2), 1473–1489. https://doi.org/10.5194/hess-22-1473-2018

Atefi, M. R., & Miura, H. (2022). Detection of Flash Flood Inundated Areas Using Relative Difference in NDVI from Sentinel-2 Images: A Case Study of the August 2020 Event in Charikar, Afghanistan. *Remote Sensing*, *14*(15), Article 15. https://doi.org/10.3390/rs14153647

Aubrecht, C., Özceylan, D., Steinnocher, K., & Freire, S. (2013). Multi-level geospatial modeling of human exposure patterns and vulnerability indicators. *Natural Hazards*, *68*(1), 147–163. https://doi.org/10.1007/s11069-012-0389-9

Aulady, M. F. N., Nuciferani, F. T., & Agustin, N. (2022). PENYEBAB DAN ALTERNATIF MITIGASI BENCANA BANJIR DI GRESIK SELATAN. *Bearing : Jurnal Penelitian Dan Kajian Teknik Sipil*, *7*(3), Article 3. https://doi.org/10.32502/jbearing.4648202273

Avila-Aceves, E., Plata-Rocha, W., Monjardin-Armenta, S. A., & Rangel-Peraza, J. G. (2023). Geospatial modelling of floods: A literature review. *Stochastic Environmental Research and Risk Assessment*, *37*(11), 4109–4128. https://doi.org/10.1007/s00477-023-02505-1

Cahyono, B. E., Cahyatri, P., Purwandari, E., Misto, & Febrianti, N. (2021). Mapping flooded risk area in East Java Indonesia using remote sensing data. *Journal of Physics: Conference Series*, *1825*(1), 012081. https://doi.org/10.1088/1742-6596/1825/1/012081

Calvin, K., Dasgupta, D., Krinner, G., Mukherji, A., Thorne, P. W., Trisos, C., Romero, J., Aldunce, P., Barrett, K., Blanco, G., Cheung, W. W. L., Connors, S., Denton, F., Diongue-Niang, A., Dodman, D., Garschagen, M., Geden, O., Hayward, B., Jones, C., … Péan, C. (2023). *IPCC, 2023: Climate Change 2023: Synthesis Report. Contribution of Working Groups I, II and III to the Sixth Assessment Report of the Intergovernmental Panel on Climate Change [Core Writing Team, H. Lee and J. Romero (eds.)]. IPCC, Geneva, Switzerland.* (First). Intergovernmental Panel on Climate Change (IPCC). https://doi.org/10.59327/IPCC/AR6-9789291691647

Cao, A., Esteban, M., Valenzuela, V. P. B., Onuki, M., Takagi, H., Thao, N. D., & Tsuchiya, N. (2021). Future of Asian Deltaic Megacities under sea level rise and land subsidence: Current adaptation pathways for Tokyo, Jakarta, Manila, and Ho Chi Minh City. *Current Opinion in Environmental Sustainability*, *50*, 87–97. https://doi.org/10.1016/j.cosust.2021.02.010

Castaneda, R., Garcia-Sucerquia, J., & Doblas, A. (2021). Speckle noise reduction in coherent imaging systems via hybrid median–mean filter. *Optical Engineering*, *60*(12), 123107. https://doi.org/10.1117/1.OE.60.12.123107

Chaussard, E., Amelung, F., Abidin, H., & Hong, S.-H. (2013). Sinking cities in Indonesia: ALOS PALSAR detects rapid subsidence due to groundwater and gas extraction. *Remote Sensing of Environment*, *128*, 150–161. https://doi.org/10.1016/j.rse.2012.10.015

Chen, S.-W. (2020). SAR Image Speckle Filtering With Context Covariance Matrix Formulation and Similarity Test. *IEEE Transactions on Image Processing*, *29*, 6641–6654. https://doi.org/10.1109/TIP.2020.2992883

Chini, M., Hostache, R., Giustarini, L., & Matgen, P. (2017). A Hierarchical Split-Based Approach for Parametric Thresholding of SAR Images: Flood Inundation as a Test Case. *IEEE Transactions on Geoscience and Remote Sensing*, *55*(12), 6975–6988. IEEE Transactions on Geoscience and Remote Sensing. https://doi.org/10.1109/TGRS.2017.2737664

Djalante, R. (2018). Review article: A systematic literature review of research trends and authorships on natural hazards, disasters, risk reduction and climate change in Indonesia. *Natural Hazards and Earth System Sciences*, *18*(6), 1785–1810. https://doi.org/10.5194/nhess-18-1785-2018

Eccles, R., Zhang, H., & Hamilton, D. (2019). A review of the effects of climate change on riverine flooding in subtropical and tropical regions. *Journal of Water and Climate Change*, *10*(4), 687–707. https://doi.org/10.2166/wcc.2019.175

Erkens, G., Bucx, T., Dam, R., de Lange, G., & Lambert, J. (2015). Sinking coastal cities. *Proceedings of IAHS*, *372*, 189–198. https://doi.org/10.5194/piahs-372-189-2015

Farhadi, H., Ebadi, H., Kiani, A., & Asgary, A. (2024). A novel flood/water extraction index (FWEI) for identifying water and flooded areas using sentinel-2 visible and near-infrared spectral bands. *Stochastic Environmental Research and Risk Assessment*, *38*(5), 1873–1895. https://doi.org/10.1007/s00477-024-02660-z

Farhadi, H., Ebadi, H., Kiani, A., & Asgary, A. (2025). Introducing a new index for flood mapping using Sentinel-2 imagery (SFMI). *Computers & Geosciences*, *194*, 105742. https://doi.org/10.1016/j.cageo.2024.105742

Fristyananda, M. A., & Idajati, H. (2017). Tingkat Bahaya Bencana Banjir di Kali Lamong Kabupaten Gresik. *Jurnal Teknik ITS*, *6*(1), 56–59. https://doi.org/10.12962/j23373539.v6i1.22103

Grimaldi, S., Li, Y., Pauwels, V. R. N., & Walker, J. P. (2016). Remote Sensing-Derived Water Extent and Level to Constrain Hydraulic Flood Forecasting Models: Opportunities and Challenges. *Surveys in Geophysics*, *37*(5), 977–1034. https://doi.org/10.1007/s10712-016-9378-y

Guo, J., Luan, Y., Li, Z., Liu, X., Li, C., & Chang, X. (2021). Mozambique Flood (2019) Caused by Tropical Cyclone Idai Monitored From Sentinel-1 and Sentinel-2 Images. *IEEE Journal of Selected Topics in Applied Earth Observations and Remote Sensing*, *14*, 8761–8772. IEEE Journal of Selected Topics in Applied Earth Observations and Remote Sensing. https://doi.org/10.1109/JSTARS.2021.3107279

Hariadi, M. H., Van Der Schrier, G., Steeneveld, G.-J., Sutanto, S. J., Sutanudjaja, E., Ratri, D. N., Sopaheluwakan, A., & Klein Tank, A. (2024). A high-resolution perspective of extreme rainfall and river flow under extreme climate change in Southeast Asia. *Hydrology and Earth System Sciences*, *28*(9), 1935–1956. https://doi.org/10.5194/hess-28-1935-2024

Hirabayashi, Y., Mahendran, R., Koirala, S., Konoshima, L., Yamazaki, D., Watanabe, S., Kim, H., & Kanae, S. (2013). Global flood risk under climate change. *Nature Climate Change*, *3*(9), 816–821. https://doi.org/10.1038/nclimate1911

Karnaji, K., Susanti, E., Ariadi, S., & Saud, M. (2024). Social impacts and post-disaster management in disaster-prone areas of East Java, Indonesia. *Jamba : Journal of Disaster Risk Studies*, *16*(1), 1747. https://doi.org/10.4102/jamba.v16i1.1747

Kim, J., Kim, H., Kim, D., Song, J., & Li, C. (2022). Deep Learning-Based Flood Area Extraction for Fully Automated and Persistent Flood Monitoring Using Cloud Computing. *Remote Sensing*, *14*(24), Article 24. https://doi.org/10.3390/rs14246373

Klemas, V. (2014). Remote Sensing of Floods and Flood-Prone Areas: An Overview. *Journal of Coastal Research*, *31*(4), 1005–1013. https://doi.org/10.2112/JCOASTRES-D-14-00160.1

Kuenzer, C., Guo, H., Huth, J., Leinenkugel, P., Li, X., & Dech, S. (2013). Flood Mapping and Flood Dynamics of the Mekong Delta: ENVISAT-ASAR-WSM Based Time Series Analyses. *Remote Sensing*, *5*(2), Article 2. https://doi.org/10.3390/rs5020687

Kupidura, P. (2016). COMPARISON OF FILTERS DEDICATED TO SPECKLE SUPPRESSION IN SAR IMAGES. *The International Archives of the Photogrammetry, Remote Sensing and Spatial Information Sciences*, *XLI-B7*, 269–276. XXIII ISPRS Congress, Commission VII (Volume XLI-B7) - 12–19 July 2016, Prague, Czech Republic. https://doi.org/10.5194/isprs-archives-XLI-B7-269-2016

Li, Z., Xu, S., & Weng, Q. (2024). Beyond clouds: Seamless flood mapping using Harmonized Landsat and Sentinel-2 time series imagery and water occurrence data. *ISPRS Journal of Photogrammetry and Remote Sensing*, *216*, 185–199. https://doi.org/10.1016/j.isprsjprs.2024.07.022

Loo, Y. Y., Billa, L., & Singh, A. (2015). Effect of climate change on seasonal monsoon in Asia and its impact on the variability of monsoon rainfall in Southeast Asia. *Geoscience Frontiers*, *6*(6), 817–823. https://doi.org/10.1016/j.gsf.2014.02.009

Luu, C., Tran, H. X., Pham, B. T., Al-Ansari, N., Tran, T. Q., Duong, N. Q., Dao, N. H., Nguyen, L. P., Nguyen, H. D., Thu Ta, H., Le, H. V., & Meding, J. von. (2020). Framework of Spatial Flood Risk Assessment for a Case

Study in Quang Binh Province, Vietnam. *Sustainability*, *12*(7), Article 7. https://doi.org/10.3390/su12073058

Malinowski, R., Groom, G., Schwanghart, W., & Heckrath, G. (2015). Detection and Delineation of Localized Flooding from WorldView-2 Multispectral Data. *Remote Sensing*, *7*(11), Article 11. https://doi.org/10.3390/rs71114853

Marfai, M. A., Sekaranom, A. B., & Ward, P. (2015). Community responses and adaptation strategies toward flood hazard in Jakarta, Indonesia. *Natural Hazards*, *75*(2), 1127–1144. https://doi.org/10.1007/s11069-014-1365-3

Martinis, S., & Rieke, C. (2015). Backscatter Analysis Using Multi-Temporal and Multi-Frequency SAR Data in the Context of Flood Mapping at River Saale, Germany. *Remote Sensing*, *7*(6), Article 6. https://doi.org/10.3390/rs70607732

Munawar, H. S., Hammad, A. W. A., & Waller, S. T. (2022). Remote Sensing Methods for Flood Prediction: A Review. *Sensors*, *22*(3), Article 3. https://doi.org/10.3390/s22030960

Muñoz, D. F., Muñoz, P., Moftakhari, H., & Moradkhani, H. (2021). From local to regional compound flood mapping with deep learning and data fusion techniques. *Science of The Total Environment*, *782*, 146927. https://doi.org/10.1016/j.scitotenv.2021.146927

Nadzir, Z. A., Simarmata, N., & Aliffia, A. (2020). PENGEMBANGAN ALGORITMA IDENTIFIKASI SAWAH PADI BERDASARKAN SPEKTRA FASE PADI (STUDI KASUS: LAMPUNG SELATAN) (Paddy Field Identification Algorithm Development Using Spectral Value of Paddy Field (Case Study: South Lampung)). *JURNAL SAINS INFORMASI GEOGRAFIS*, *3*(1), 23. https://doi.org/10.31314/jsig.v3i1.537

Nasution, B. I., Saputra, F. M., Kurniawan, R., Ridwan, A. N., Fudholi, A., & Sumargo, B. (2022). Urban vulnerability to floods investigation in jakarta, Indonesia: A hybrid optimized fuzzy spatial clustering and news media analysis approach. *International Journal of Disaster Risk Reduction*, *83*, 103407. https://doi.org/10.1016/j.ijdrr.2022.103407

Nguyen, T. H., Ricci, S., Fatras, C., Piacentini, A., Delmotte, A., Lavergne, E., & Kettig, P. (2022). Improvement of Flood Extent Representation With Remote Sensing Data and Data Assimilation. *IEEE Transactions on Geoscience and Remote Sensing*, *60*, 1–22. IEEE Transactions on Geoscience and Remote Sensing. https://doi.org/10.1109/TGRS.2022.3147429

Nicholls, R. J., Lincke, D., Hinkel, J., Brown, S., Vafeidis, A. T., Meyssignac, B., Hanson, S. E., Merkens, J.-L., & Fang, J. (2021). A global analysis of subsidence, relative sea-level change and coastal flood exposure. *Nature Climate Change*, *11*(4), 338–342. https://doi.org/10.1038/s41558-021-00993-z

Pusat Krisis Kesehatan. (2022). *Informasi Awal Banjir di 1 Kecamatan, GRESIK, JAWA-TIMUR*. Kementerian Kesehatan Republik Indonesia. https://pusatkrisis.kemkes.go.id/Banjir-di-GRESIK-JAWA-TIMUR-06-07-2022-90

Rahman, Md. S., & Di, L. (2017). The state of the art of spaceborne remote sensing in flood management. *Natural Hazards*, *85*(2), 1223–1248. https://doi.org/10.1007/s11069-016-2601-9

Rehman, S., Sahana, M., Hong, H., Sajjad, H., & Ahmed, B. B. (2019). A systematic review on approaches and methods used for flood vulnerability assessment: Framework for future research. *Natural Hazards*, *96*(2), 975–998. https://doi.org/10.1007/s11069-018-03567-z

Rosser, J. F., Leibovici, D. G., & Jackson, M. J. (2017). Rapid flood inundation mapping using social media, remote sensing and topographic data. *Natural Hazards*, *87*(1), 103–120. https://doi.org/10.1007/s11069-017-2755-0

Sadiq, R., Akhtar, Z., Imran, M., & Ofli, F. (2022). Integrating remote sensing and social sensing for flood mapping. *Remote Sensing Applications: Society and Environment*, *25*, 100697. https://doi.org/10.1016/j.rsase.2022.100697

Santoso, E. B. (2013). MANAJEMEN RISIKO BENCANA BANJIR KALI LAMONG PADA KAWASAN PERI-URBAN SURABAYA-GRESIK MELALUI PENDEKATAN KELEMBAGAAN. *Jurnal Penataan Ruang*, *8*(2).

Sari, O. L., Yanti, R. M. K., Fauzi, A., & Patabang, A. M. P. (2021). Effect of flood risk management methods on urban flooding: Article review. *Teknika: Jurnal Sains Dan Teknologi*, *17*(2), 301. https://doi.org/10.36055/tjst.v17i2.12455

Schnebele, E., & Cervone, G. (2013). Improving remote sensing flood assessment using volunteered geographical data. *Natural Hazards and Earth System Sciences*, *13*(3), 669–677. https://doi.org/10.5194/nhess-13-669-2013

Schumann, G. J.-P., & Moller, D. K. (2015). Microwave remote sensing of flood inundation. *Physics and Chemistry of the Earth, Parts A/B/C*, *83–84*, 84–95. https://doi.org/10.1016/j.pce.2015.05.002

See, L. (2019). A Review of Citizen Science and Crowdsourcing in Applications of Pluvial Flooding. *Frontiers in Earth Science*, *7*. https://doi.org/10.3389/feart.2019.00044

Shofwan, M., & Prabhaswara, L. M. (2023). Karakteristik Kerentanan Banjir Di Kecamatan Driyorejo. *COMPACT: Spatial Development Journal*, *2*(1), Article 1. https://doi.org/10.35718/compact.v2i1.850

Sholichin, M., Prayogo, T. B., Hendrawan, A. P., Fidari, J. S., Hidayati, A. S. D. S. N., & Sulilo, A. A. (2024). Using hecras modeling to analysis of flood disaster at Kali Lamong, East Java. *AIP Conference Proceedings*, *3043*(1), 030002. https://doi.org/10.1063/5.0206590

Simarmata, N., Nadzir, Z. A., & Sari, D. N. (2023). Analisis Perubahan Garis Pantai menggunakan Metode Sentinel-1 Dual-Polarized Water Index (SDWI) berbasis Data Multitemporal pada Google Earth Engine. *Geomatika*, *29*(2), 107–120.

Singh, S., & Kansal, M. L. (2022). Chamoli flash-flood mapping and evaluation with a supervised classifier and NDWI thresholding using Sentinel-2 optical data in Google earth engine. *Earth Science Informatics*, *15*(2), 1073–1086. https://doi.org/10.1007/s12145-022-00786-8

Siswanto, R. D., & Puspaningtyas, A. (2023). Implementasi Kebijakan Penanggulangan Bencana dan Mitigasi Banjir di Kabupaten Gresik. *Policy and Maritime Review*, 21–31. https://doi.org/10.30649/pmr.v2i1.42

Soria-Ruiz, J., Fernandez-Ordoñez, Y. M., Ambrosio-Ambrosio, J. P., Escalona-Maurice, M. J., Medina-García, G., Sotelo-Ruiz, E. D., & Ramirez-Guzman, M. E. (2022). Flooded Extent and Depth Analysis Using Optical and SAR Remote Sensing with Machine Learning Algorithms. *Atmosphere*, *13*(11), Article 11. https://doi.org/10.3390/atmos13111852

Sun, Z., Luo, J., Yang, J., Yu, Q., Zhang, L., Xue, K., & Lu, L. (2020). Nation-Scale Mapping of Coastal Aquaculture Ponds with Sentinel-1 SAR Data Using Google Earth Engine. *Remote Sensing*, *12*(18), Article 18. https://doi.org/10.3390/rs12183086

Sy, B., Frischknecht, C., Dao, H., Consuegra, D., & Giuliani, G. (2019). Flood hazard assessment and the role of citizen science. *Journal of Flood Risk Management*, *12*(S2), e12519. https://doi.org/10.1111/jfr3.12519

Ta, L., Yu ,Chen, Li ,Zhenhong, Hu ,Xiaoning, Song ,Chuang, Huang ,Wubiao, & and Zhou, M. (2024). Dynamic flood mapping by a normalized probabilistic classification method using satellite radar amplitude time series. *GIScience & Remote Sensing*, *61*(1), 2380125. https://doi.org/10.1080/15481603.2024.2380125

Tanim, A. H., McRae, C. B., Tavakol-Davani, H., & Goharian, E. (2022). Flood Detection in Urban Areas Using Satellite Imagery and Machine Learning. *Water*, *14*(7), Article 7. https://doi.org/10.3390/w14071140

Taslyanto, C. A. P., & Deviantari, U. W. (2024). Spatial-Based Flood Susceptibility Mapping Using Analytical Hierarchy Process Techniques (Case Study: Gresik Regency). *IOP Conference Series: Earth and Environmental Science*, *1418*(1), 012037. https://doi.org/10.1088/1755-1315/1418/1/012037

Triana, Y. T., & Hidayah, Z. (2020). KAJIAN POTENSI DAERAH RAWAN BANJIR ROB DAN ADAPTASI MASYARAKAT DI WILAYAH PESISIR UTARA SURABAYA. *Juvenil:Jurnal Ilmiah Kelautan Dan Perikanan*, *1*(1), 141–150. https://doi.org/10.21107/juvenil.v1i1.6961

Twele, A., Cao ,Wenxi, Plank ,Simon, & and Martinis, S. (2016). Sentinel-1-based flood mapping: A fully automated processing chain. *International Journal of Remote Sensing*, *37*(13), 2990–3004. https://doi.org/10.1080/01431161.2016.1192304

Uddin, K., Matin, M. A., & Meyer, F. J. (2019). Operational Flood Mapping Using Multi-Temporal Sentinel-1 SAR Images: A Case Study from Bangladesh. *Remote Sensing*, *11*(13), Article 13. https://doi.org/10.3390/rs11131581

Ward, P. J., Jongman, B., Weiland, F. S., Bouwman, A., van Beek, R., Bierkens, M. F. P., Ligtvoet, W., & Winsemius, H. C. (2013). Assessing flood risk at the global scale: Model setup, results, and sensitivity. *Environmental Research Letters*, *8*(4), 044019. https://doi.org/10.1088/1748-9326/8/4/044019

Xue, W., Yang, H., Wu, Y., Kong, P., Xu, H., Wu, P., & Ma, X. (2021). Water Body Automated Extraction in Polarization SAR Images With Dense-Coordinate-Feature-Concatenate Network. *IEEE Journal of Selected*

Topics in Applied Earth Observations and Remote Sensing, *14*, 12073–12087. IEEE Journal of Selected Topics in Applied Earth Observations and Remote Sensing. https://doi.org/10.1109/JSTARS.2021.3129182

Yagoub, M. M., Alsereidi, A. A., Mohamed, E. A., Periyasamy, P., Alameri, R., Aldarmaki, S., & Alhashmi, Y. (2020). Newspapers as a validation proxy for GIS modeling in Fujairah, United Arab Emirates: Identifying flood-prone areas. *Natural Hazards*, *104*(1), 111–141. https://doi.org/10.1007/s11069-020-04161-y

Yamamoto, K., Sayama, T., & Apip. (2021). Impact of climate change on flood inundation in a tropical river basin in Indonesia. *Progress in Earth and Planetary Science*, *8*(1), 5. https://doi.org/10.1186/s40645-020-00386-4

Yin, J., Jonkman, S., Lin, N., Yu, D., Aerts, J., Wilby, R., Pan, M., Wood, E., Bricker, J., Ke, Q., Zeng, Z., Zhao, Q., Ge, J., & Wang, J. (2020). Flood Risks in Sinking Delta Cities: Time for a Reevaluation? *Earth's Future*, *8*(8), e2020EF001614. https://doi.org/10.1029/2020EF001614

Yu, Y., d'Alessandro, M. M., Tebaldini, S., & Liao, M. (2020). Signal Processing Options for High Resolution SAR Tomography of Natural Scenarios. *Remote Sensing*, *12*(10), Article 10. https://doi.org/10.3390/rs12101638

Zhao, B., Sui, H., Liu, J., Shi, W., Wang, W., Xu, C., & Wang, J. (2024). Flood inundation monitoring using multi-source satellite imagery: A knowledge transfer strategy for heterogeneous image change detection. *Remote Sensing of Environment*, *314*, 114373. https://doi.org/10.1016/j.rse.2024.114373

Zhu, X. X., & Bamler, R. (2014). Superresolving SAR Tomography for Multidimensional Imaging of Urban Areas: Compressive sensing-based TomoSAR inversion. *IEEE Signal Processing Magazine*, *31*(4), 51–58. IEEE Signal Processing Magazine. https://doi.org/10.1109/MSP.2014.2312098